Tensor Representation of Electric Machine Windings and its Connection with Winding Functions

J. Dillon Vann, *Student Member, IEEE*
University of Florida
Gainesville, FL, USA
jdillon.vann@ufl.edu

Baoyun Ge, *Member, IEEE*
Georgia Institute of Technology
Atlanta, GA, USA
baoyun.ge@ece.gatech.edu

***Abstract*—Windings are the fundamental components of electric machines. Conventional winding analysis methods or tools include slot diagrams, star diagrams, phasor diagrams, winding functions, etc. This paper presents a new tool for winding analysis that encompasses the essential idea behind these conventional methods and at the same time facilitates computations. The idea is based on the relationship among multiple concepts specifically associated with electric machine windings, including magnetic, electrical, layer, and phase orders. Such a relationship can be described through tensors. Five example windings, namely fractional slot, full-pitch, short-pitch, concentric, and hairpin windings, are presented to illustrate the proposed framework. Furthermore, we discuss how we will use this new representation method to explore new winding configurations.**

Keywords—electric machine winding, matrix, tensor, winding function

I. Introduction

Windings are the fundamental component of electric motors and generators, or collectively electric machines (EMs). Together with current excitation, they provide magnetomotive forces (MMF) that facilitate force or torque production. Windings have received research and development attention given their significant role in EMs. For example, fractional slot concentrated windings are used to significantly increase the inductance in surface permanent magnet EMs (SPMs) and thus improve their flux-weakening capability [1]. Another example is the usage of hairpin windings in interior permanent magnet EMs (IPMs) to maximize the slot-filling factor so that conduction losses are minimized [2]. Applications like drones, servos, and EVs have driven these studies.

For the purpose of designing EMs, there are four main methods of winding analysis: slot diagrams, star diagrams, phasor diagrams, and winding functions [3], [4]. They are illustrated in Fig. 1 through an example winding (18-slot, 3-phase, 2-pole, short-pitch winding). Their advantages and disadvantages are summarized below:

- a slot diagram presents the layout of coils and their interconnections clearly, but the phase relationship among coils or windings requires closely following the coil routing, which leads to the corresponding star diagram;
- a star diagram is almost the opposite of its corresponding slot diagram in terms of the information it displays. It mitigates the drawbacks of slot diagram mentioned above, but the information about coil side layout and interconnection is lost;
- a phasor diagram groups the phasors in the star diagram and aggregates them to produce the phasors for each phase. It inherits the disadvantages of the star diagram;
- a winding function encodes the layout of coil sides and the number of turns. However, similar to the star diagram, the coil side interconnection is not represented. Due to this deficiency, the same winding function may result for full-pitch, short-pitch, and concentric windings. This will be seen in the example windings presented in Sections IV, V, and VI. Nevertheless, winding functions uniquely facilitate the computation of self and mutual inductances [5].

As a result, these tools or methods are often combined to fulfill the analysis of EM windings.

This paper presents a winding representation method that encompasses the strengths of these conventional approaches while facilitating computation. The idea is based on relationships among multiple concepts specifically associated with electric machine windings, including magnetic, electrical, layer, and phase orders. These relationships can be described through tensors (generalized matrices). Five example windings are used to illustrate this representation method. Given that fractional slot and hairpin windings have been investigated

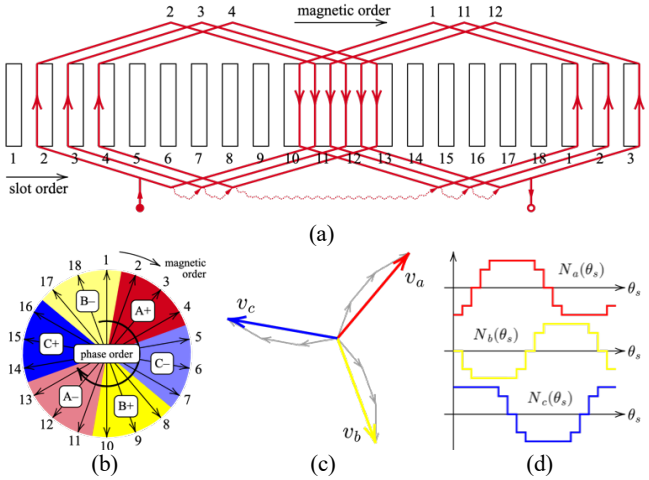

Fig. 1 Conventional winding analysis methods and tools.

This work was supported in part by the U.S. National Science Foundation Award #2338541.

extensively in recent years, they are included to illustrate the modern application of the proposed framework. It is worth noting that the idea is stemmed from [6], where only the relationship between magnetic and electrical orders is modeled.

The rest of the paper is organized as follows. Section II elaborates on the concept of magnetic, electrical, and layer order. These concepts are used in the examples to represent electric machine windings using tensors. Sections III, IV, V, VI, and VII present five example windings to demonstrate the tensor representation method across various winding types, including fractional slot, full-pitch, short-pitch, concentric, and hairpin windings. Given the recent research attention, fractional slot winding and hairpin winding will be primary areas of discussion. Applying the new representation method to hairpin windings requires an additional layer of complexity to accommodate layer orders in hairpin windings. Lastly, Sections VIII and IX respectively outline plans for future work and conclude the contribution.

II. The Concept of Magnetic, Electrical, and Layer Orders

A. Magnetic Order and Star Diagrams

The concept of magnetic order concerns coil sides. As the rotor in an EM revolves, the flux path rotates as well. The coil sides on the stator thus cut through the field lines. The induced back-electromotive force (back-EMF) will have phase relations according to the circumferential positions of coil sides. Such a sequence in back-EMF is the magnetic order. Referring to Fig. 1b, a star diagram reflects the magnetic order when phasors account for coil sides instead of coils.

B. Electrical Order and Slot Diagram

The concept of electrical order concerns the polarities of coil sides or coils when they are used to form coils or windings respectively. Since only one current direction is possible at any instant in a coil or a winding, the current polarities of their constitutive components are forced. Referring to Fig. 1 (a), this is reflected in a slot diagram through the arrows. Notice that all arrows in one winding can be flipped simultaneously according to the preferred polarity convention.

C. Layer Order

In conventional windings with two layers, a coil usually consists of one coil side from the upper layer and another coil side from the lower layer. This practice balances out mismatching of back-EMF induced in these two layers, therefore there is no need to distinguish the two layers in the presented tensor representation. However, this is not the case for hairpin windings whose layers are often more than two. To distinguish layers in such windings, we increase the rank of tensors from 2 (matrices) to 3; the third rank denotes layers.

III. Example 1: Fractional Slot Winding

Figure 2 shows a slot diagram for a 3 phase, 12 slot, 10 pole, fractional slot, concentrated winding [1]. In distributed windings, the number of slots is an integer multiple of the number of poles. Fractional slot windings do not abide by this

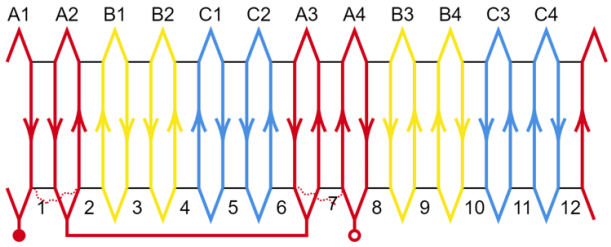

Fig. 2 Slot diagram of a fractional slot winding [1].

regularity. This said, the number of slots must be a multiple of the number of phases. In this winding, the slot per pole per phase (SPP) is 2/5, which meets the definition. For clarity, the slots are labeled 1-12 and the coils are labeled A1-C4. The span of each coil is one slot. For example, coil A2 has one coil side in slot 1 and the other coil side in slot 2. Furthermore, adjacent coils from the same phase belt may have current flow in opposite directions (*e.g.* A1 and A2). These concepts and characteristics of the windings are to be clearly present in our tensor representation.

The rank 2 tensors (*i.e.* matrices) shown in Fig. 3 are an exact and computationally friendly method of representing all the details from the slot diagram shown in Fig. 2. As discussed, the winding has coils that span one slot and either carries counterclockwise or clockwise currents. Tensor C_1 in Fig. 3 (a) is rank 2 (*i.e.* a matrix) and documents the relationship between magnetic order and electrical order. Magnetic order is mapped directly to the slots on the winding diagram. For example, magnetic order 1 represents the first slot, magnetic order 2 represents the second slot, etc. The electrical order is a strategically chosen sequence of the coils in the winding. When the electrical order is chosen carefully, C_1 has an intuitive appearance that may provide new insight into the winding pattern. For this winding, the electrical order starts with the coil that begins in slot 1 and ends in slot 2 (*i.e.* coil A2). Using the magnetic order or slot number as a reference, this is the first coil that does not wrap across the boundary (between slot 12 and slot 1). Using Fig. 2, the electrical order convention then progresses from left to right until it ends with coil A1 (*i.e.* A2, B1, B2, C1, C2, A3, A4, B3, B4, C3, C4, A1). Note this concept is not directly tied to the slot diagram, it is simply a strategic naming convention for the coils.

To create C_1, it is necessary to understand the meaning of the '1's and '-1's. In C_1, a '1' represents the first side of the coil, and a '-1' represents the second side of the coil. The tensor C_1 does

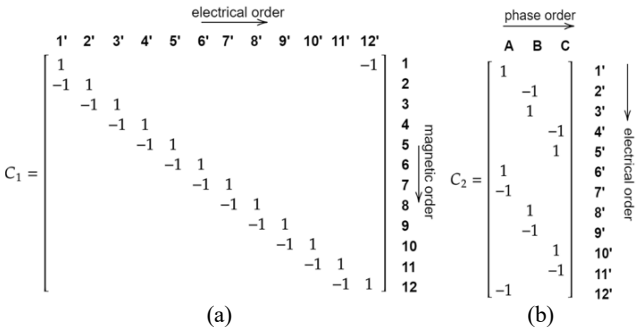

Fig. 3 Tensor representation of the fractional slot winding in Fig. 2.

not encode current direction, it simply assembles the coil sides into coils and puts them in a strategically chosen order called electrical order. For the fractional slot winding in Fig. 2, the chosen electrical order allowed each vertical pair of '1' and '-1' to shift down by one slot for each progression in electrical order.

The tensor C_2 (also rank 2, *i.e.* a matrix), shown in Fig. 3(b), registers how coils are assembled into phase windings. It accounts for the direction of current and phase order. Specifically, C_2 shows whether a coil is connected in a reverse direction and thus carries a current flowing in the opposite direction. The convention used in this paper is that counterclockwise currents are represented by '1's and clockwise currents are represented by '-1's. This is a chosen convention and can be reversed if advantageous for the problem. In most applications, this decision does not hold much weight. For this winding and corresponding C_2, the coils flip back and forth between counterclockwise and clockwise currents 6 times. Hence, C_2 will alternate between 1 and -1 except between pairs 5/6 and 11/12.

magnetic order

	1'	2'	3'	4'	5'	6'	7'	8'	9'	10'	11'	12'	
$(C_1C_2)^T =$	2	−1				1	−2	1				−1	A
		−1	2	−1				1	−2	1			B
				−1	2	−1				1	−2	1	C

phase order

Fig. 4 Resultant of matrix multiplication of C_1 and C_2 namely C_1C_2.

The multiplication of tensors C_1 and C_2 delivers the most powerful aspect of the tensor representation. In this paper, we will denote the resultant tensor of this multiplication as C_1C_2. Figure 4 presents C_1C_2 for this fractional-slot winding. Notice that Fig. 4 has been transposed for display. In fact, C_1C_2 shows the differential of the winding function, meaning the cumulative sum of C_1C_2 down a phase will match the winding function shape. To match exactly, it must be shifted vertically to have an average of zero, as the definition of the winding function [7].

In this problem, the current flowing downward in Fig. 2 is taken as a positive change in the winding function and the current flowing upward in Fig. 2 is a negative change. As one progresses across the slots or magnetic order, one will notice that slots covered by the same phase belt will have a 2 or -2. If the absolute value of each cell in tensor C_1C_2 is taken, the sum of each column will be 2. This intuitively makes sense because there are 2 coil sides on each slot. These patterns highlight the intuitive nature of the tensor representation method.

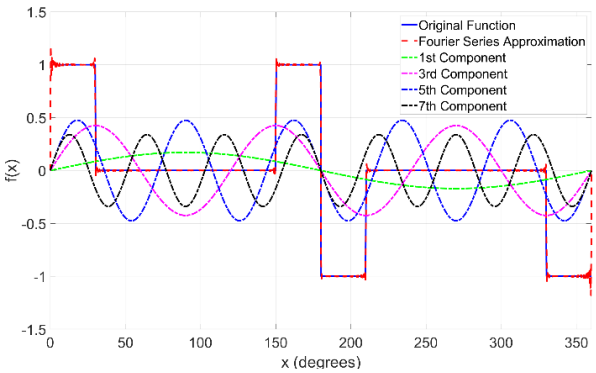

Fig. 5 Phase A winding function of the fractional-slot winding with Fourier approximation and graphed 1st, 3rd, 5th, and 7th harmonics.

Figure 5 displays the winding function of phase A or the cumulative sum of the phase A row in $(C_1C_2)^T$ with the proper vertical shift. The Fourier series expansion of the winding function (the first 4 odd harmonics) is also overlaid. Figure 6 shows the Fourier series spectrum. As expected for a 10 pole machine, the 5th harmonic is the biggest component.

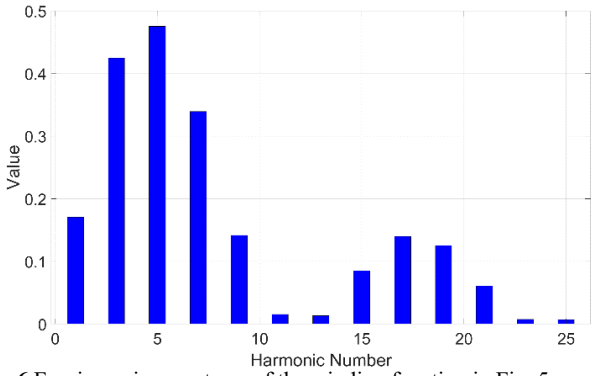

Fig. 6 Fourier series spectrum of the winding function in Fig. 5

IV. Example 2: Distributed Full-Pitch Winding

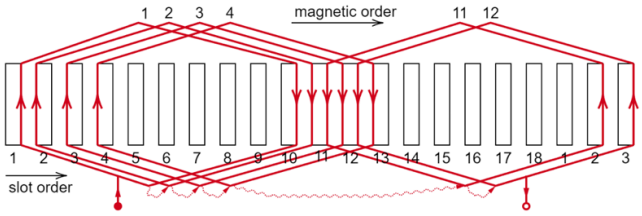

Fig. 7 Slot diagram for a distributed full-pitch winding.

The slot diagram in Fig. 7 is for a 3 phase, 18 slot, 2 pole, full-pitch winding. Because it is 18 slots, 2 pole, and full-pitch, each coil spans 180 mechanical degrees or 9 slots. Hence, the top side of this diagram will connect coil sides with 9 slots between them. For example, the coil side in slot 1 is connected to a coil side in slot 10; this is repeated for the rest of the coil sides. It is important to also notice that there are 4 coils on the left side of the diagram and 2 coils on the right side of the diagram. The left 4 are connected reversely to the coils on the right. This will be reflected in the C_2 tensor.

Tensor C_1 connects the coil sides so that there are 9 slots between them. The electrical order convention for this winding is identical to the convention for fractional slot windings. The electrical order begins with the first full coil that does not wrap around the boundary: the coil with a '1' in row 1 and '-1' in row 10. Referencing Fig. 7, the electrical order progresses from left to right. The final coil, which begins in slot 18 and finishes in slot 9, has a '1' in row 18 and '-1' in row 9. This pattern facilitates the construction of C_1.

Understanding the shifts between phases is crucial for constructing C_2. Phase B and phase C are shifted 6 slot forward and backward from phase A, respectively. The shift is 6 slots

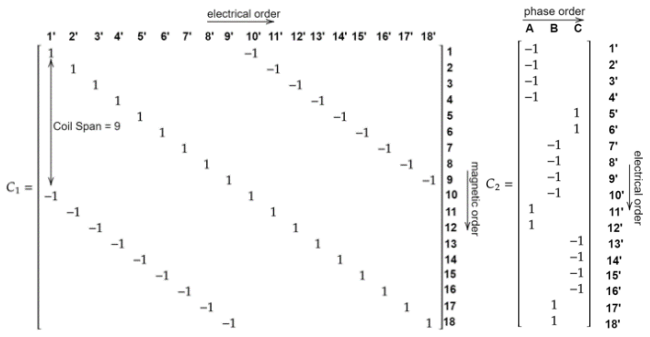

(a) (b)

Fig. 8 Tensor representation of the full-pitch winding in Fig. 7

because there are 18 slots, 1 pole pair, and 3 phases ($\frac{18\ slots}{3\ phases * 1\ pole\ pair} = 6$). It is necessary to recognize the base pattern of connections for the coils: the first four coils are connected so that the current flows clockwise and the final 2 coils are connected so that the current flows counterclockwise. C_2 can be constructed by reflecting this pattern with the 6-slot shift between phases.

The multiplication of these rank 2 tensors will be discussed in section VI. The full-pitch winding and the next two example windings have the same winding function so their C_1C_2 resultant tensors will be identical. The main differences among them are how the coil sides and coils are connected, which are reflected in C_1 and C_2.

V. Example 3: Distributed Short-Pitch Winding

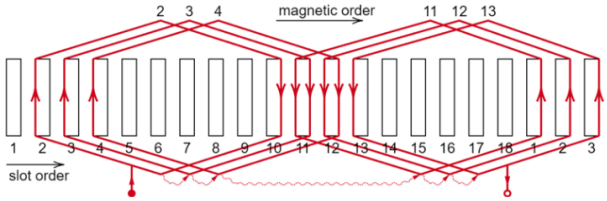

Fig. 9 Slot diagram for a distributed short-pitch winding.

This winding is a 3 phase, 18 slot, 2 pole, short-pitch winding. It is similar to the previous winding except there is a small change in the connections of the coil sides. It is short pitched by 20 degrees, or equivalently the coil span is 160 degrees. The pitch is $\frac{8}{9} = \frac{160°}{180°}$, meaning that there will be 8 slots between each coil side instead of 9. This causes one of the clockwise coils to flip and be connected counterclockwise. These changes are reflected in the tensors C_1 and C_2.

Now there are only 8 slots between the '1's and '-1's in C_1, reflecting the short-pitched nature of the winding. Comparing to Fig. 8b, C_2 shows that one of the clockwise coils is connected counterclockwise; hence, there are groups of three '1's and three '-1's. Because the shifts between phases are the same, the 6 slot gaps between the '1's and '-1's are still present. The differences between the full-pitch winding and the short-pitch winding are subtle but clearly captured in the tensor representation.

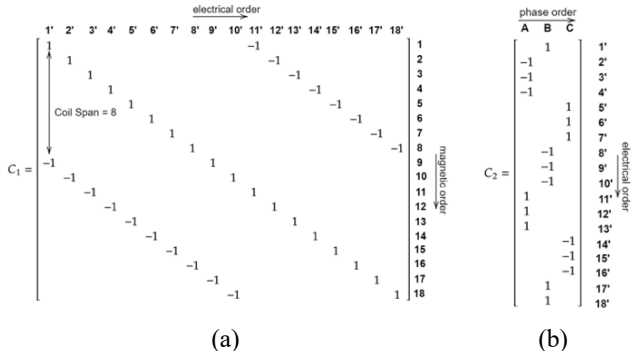

(a) (b)

Fig. 10 Tensor representation of the short-pitch winding in Fig. 9.

VI. Example 4: Concentric Winding

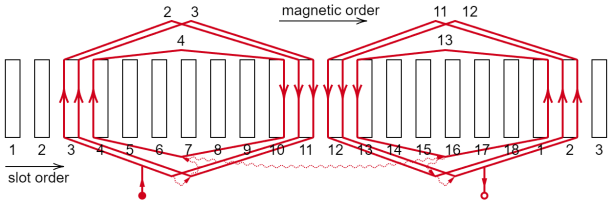

Fig. 11 Slot diagram for a distributed short-pitch winding.

The winding in Fig. 11 is a 3 phase, 18 slot, 2 pole, concentric winding. The concentric winding is quite different than the full-pitch and short-pitch winding. A concentric winding wraps inward on itself. This creates the two independent sections of coils seen in the slot diagram in Fig. 11: one section with counterclockwise coils and one section with clockwise coils. This slot diagram only has one phase, so there will be six independent sections of coils in the full, 3-phase, slot diagram. These independent sections are reflected in both C_1 and C_2 as well.

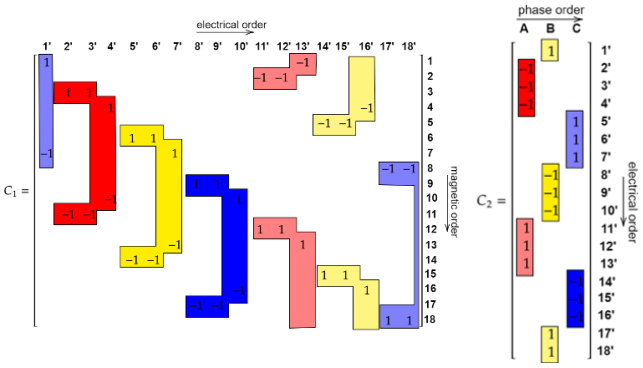

(a) (b)

Fig. 12 Tensor representation of the short-pitch winding in Fig. 11.

This tensor C_1 may be the most interesting one discussed thus far. The phases have been highlighted and color-coded for clarity. The red regions are for phase A, the yellow regions are for phase B, and the blue regions are for phase C. There are 6 semicircular regions in C_1, two for each phase. This semicircular shape reflects the inward wrapping of the concentric winding slot diagram. Tensor C_2 for the concentric winding (Fig. 12b) is the same as that for the short-pitch winding (Fig. 10b). This observation indicates there are underlying similarities in their

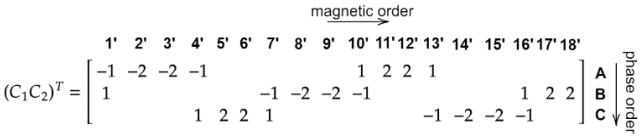

Fig. 13 Resultant from multiplication of C_1 and C_2 for the full-pitch, short-pitch, and concentric windings (transposed).

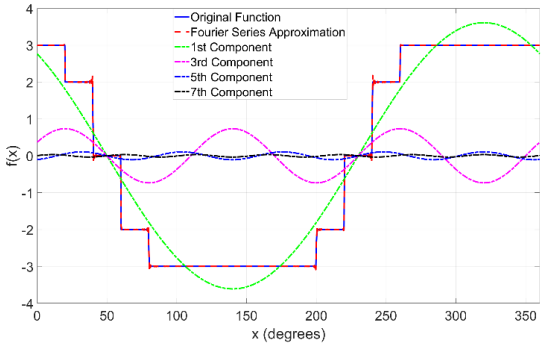

Fig. 14 Phase A winding function of the full-pitch, short-pitch, and concentric winding with Fourier approximation and harmonics.

designs. Both the short-pitch winding and concentric winding have 3 clockwise and 3 counterclockwise connected coils; both have 6 slots between phases.

Next, the resultant tensor for the full-pitch, short-pitch, and concentric winding will be presented. Although the full-pitch, short-pitch, and concentric windings have shown a considerable amount of differentiation in slot diagram as well as C_1 and C_2, each product of C_1 and C_2 results in the same tensor shown in Fig. 13. This inherently means that their winding functions are all the same and their only differences are in the method of coil construction and coil interconnection.

The cumulative sum of the phase A row results in the winding function shown in Fig. 14. Again, this validates the accuracy and applicability of the tensor representation method. Fig. 15 shows the Fourier series spectrum for the winding function in Fig. 14. As expected, the 1st harmonic or the fundamental component has the highest amplitude.

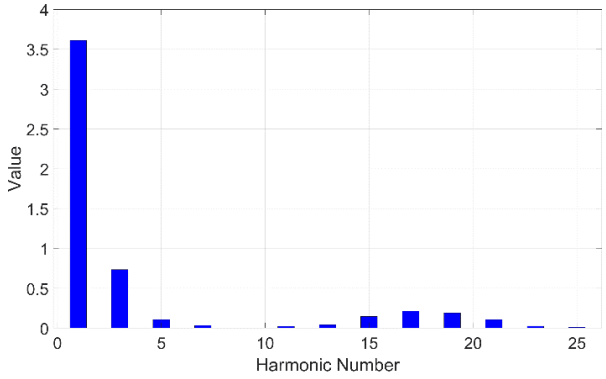

Fig. 15 Fourier series spectrum of the winding function in Fig. 14.

VII. Example 5: Haripin Winding

Figure 16 on the next page shows the slot diagram for a 24 slot, 4 pole, 4 layer hairpin winding [8]. Only phase A coils, connections, and terminals are depicted to avoid crowdedness.

Layers in hairpin windings present an additional complication to the tensor representation method. This complication is handled by increasing the rank of the tensors from rank 2 to rank 3. The slot diagram displays the layering through the vertical lines that are drawn on each slot. The left most solid line is the first layer, the dashed line is the second layer, the dotted line is the third layer, and the rightmost solid line is the fourth layer. This slot diagram shows that there are four groups of pins, which is expected considering it is a 4 pole machine.

Fig. 17 shows a rank 3 C_1 tensor. Displaying rank 3 tensors on paper is not straightforward; hence a graphical approach is used in this paper. Each pin represents one element of the electrical order and is allocated an individual matrix (a slide of the rank 3 tensor). Each matrix registers one coil: layer order (horizontal) by magnetic order (vertical). Multiplication of rank 3 tensors (known as tensor product [9]) works in a similar way as the multiplication of matrices except for an important difference. The ranks of the rank 3 tensors that are multiplied must be specified. In this case, just like in the previous examples, the electrical order rank needs to be multiplied for it to collapse out of the resultant tensor. This is possible by specifying that the electrical order ranks are being multiplied in the tensor multiplication of C_1 and C_2. In this case, C_1 times C_2 still produces the winding function. The winding functions for phase A, phase B, and phase C are shown in the C_1C_2 tensor in Fig. 18.

Fig. 19 shows the winding function of the hairpin winding. It also has the Fourier series approximation and the first 4 harmonic components. Fig. 20 shows the Fourier series spectrum of the winding function in Fig. 19.

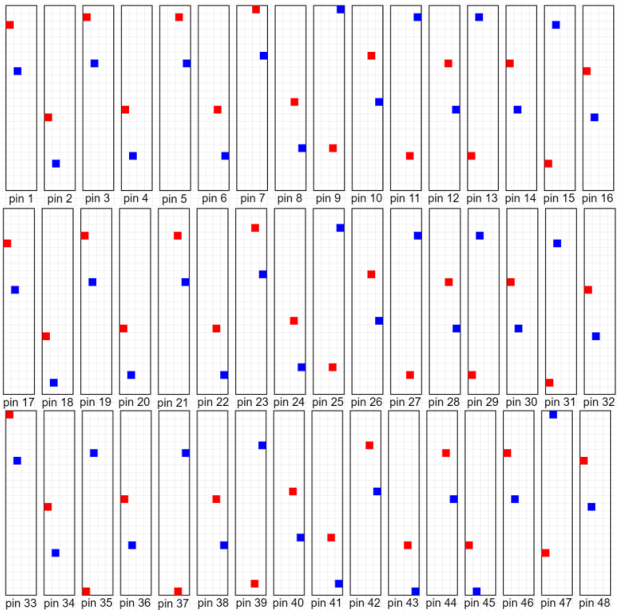

Fig. 17 Rank 3 C_1 tensor for the hairpin winding in Fig. 16.

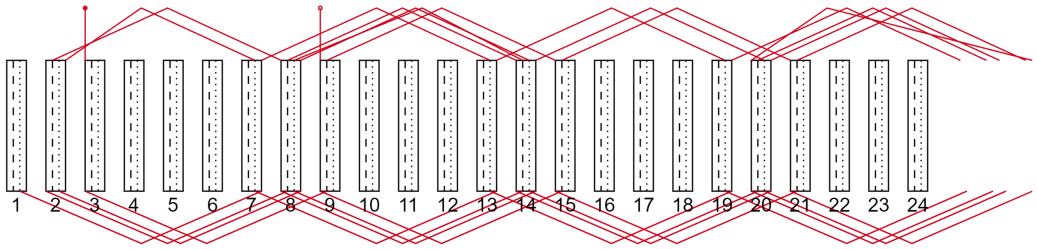

Fig. 16 Slot diagram for a hairpin winding [8].

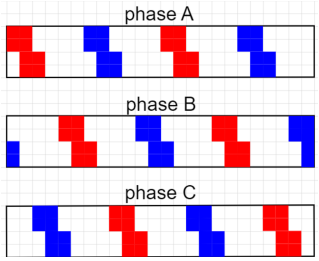

Fig. 18 Transposed rank 3 C_1C_2 tensor for the hairpin winding in Fig. 16.

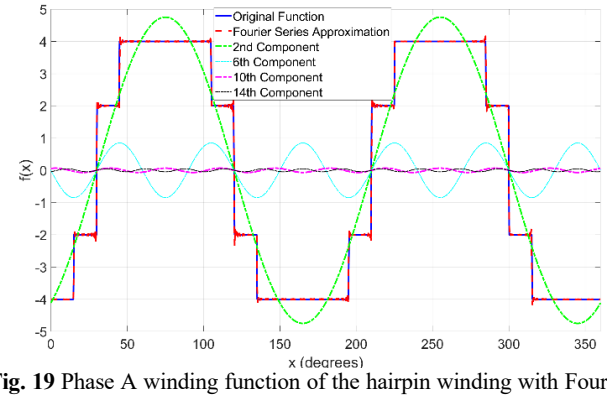

Fig. 19 Phase A winding function of the hairpin winding with Fourier approximation and harmonics.

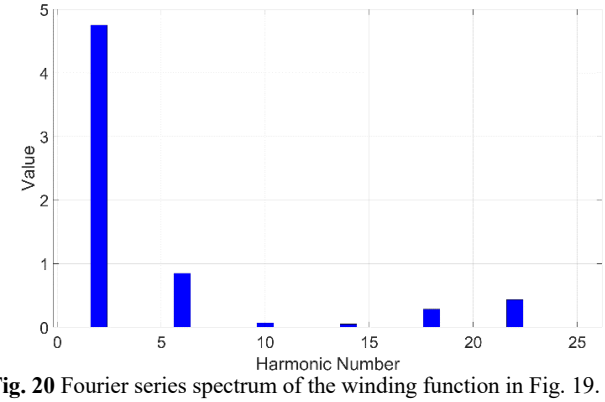

Fig. 20 Fourier series spectrum of the winding function in Fig. 19.

VIII. Future Work

One of the advantages of the new tensor representation is that it facilitates computation directly. The four existing tools/methods presented in Fig. 1 may be categorized as winding *analysis* tools. The proposed tensor tool sheds light on winding *synthesis*, where novel winding configurations are to be explored.

Through the five example windings, it has been clear that only '1's, '0's, and '-1's will show up in C_1 and C_2 to describe the relationship among magnetic, electrical, layer, and phase orders. This characteristic lends itself to computer programming and thus exploration of new windings. It is worth noting that in our presentation, turns numbers have been omitted and they can be encoded in C_1 if necessary. For most electric machines, however, all coils have the same number of turns and this information can be hidden by normalizing C_1.

Furthermore, the tensor C_1C_2 is closely related to winding function (one-to-one mapping). This enables the quick evaluation of winding configurations without resorting to existing tools/methods in Fig. 1.

Our next step in this research thrust is to design algorithms that can efficiently explore high-performance winding configurations. We may convert the winding exploration problem into a combination of an exact cover problem [10] from computer science and an optimization problem. The goal is to fill C_1 and C_2 with '1's, '0's, and '-1's to maximize pre-determined objective functions. The number of options filling C_1 and C_2 is limited due the following constraints (using rank 2 tensors as an example): (1) each column of C_1 contains exactly one '1' and one '-1'; (2) the sum of the absolute value of each row of C_1 equals number of layers; (3) the sum of the absolute value of each row of C_2 equals number of layers; (4) the sum of each column of C_1C_2 is zero; (5) columns of C_2 and C_1C_2 are circular shift of each other. The objective of the exploration can be high fundamental component, lower total harmonic distortion, end winding length, etc., or a combination of them. The corresponding objective function can be obtained via the postprocessing of C_1, C_2, and C_1C_2.

IX. Conclusions

This paper has introduced a new method of representation for EM windings. It has been applied to five different example windings: fraction-slot winding; full-pitch, distributed winding; short-pitch, distributed winding; concentric winding; and hairpin winding. The first four types of windings were represented with rank 2 tensors, namely C_1 and C_2. The hairpin winding involves non-identical layers which necessitate an extra rank to encode the layer information. Hence, the hairpin winding is represented with rank 3 tensors. For all of these windings, the C_1 and C_2 tensors can be multiplied to create a third tensor called C_1C_2, which interestingly encodes the differential of the winding function. We also presented Fourier analysis for all winding functions, demonstrating how the new representation method

encompasses the advantages of existing tools/methods for winding analysis.

Furthermore, we further discussed how the new winding representation approach can be useful in exploring novel windings, which has been largely relied on EM designers' intuition. The fact that C_1 and C_2 are filled '1's, '0's, and '-1's lends itself to computer programming. The relationship between C_1C_2 and winding function facilitates straightforward evaluation of winding configurations. We will explore this opportunity in a follow-up work.

ACKNOWLEDGMENT

The author J. Dillon Vann would like to thank Dr. Harley for providing supporting knowledge for the work. The author Baoyun Ge would like to thank the Department of Electrical and Computer Engineering at the University of Florida, where he prepared the presented work.

REFERENCES

[1] A. M. EL-Refaie, "Fractional-Slot Concentrated-Windings Synchronous Permanent Magnet Machines: Opportunities and Challenges," *IEEE Trans. Ind. Electron.*, vol. 57, no. 1, pp. 107–121, Jan. 2010, doi: 10.1109/TIE.2009.2030211.

[2] T. Zou *et al.*, "A Comprehensive Design Guideline of Hairpin Windings for High Power Density Electric Vehicle Traction Motors," *IEEE Trans. Transp. Electrification*, vol. 8, no. 3, pp. 3578–3593, Sep. 2022, doi: 10.1109/TTE.2022.3149786.

[3] T. A. Lipo, *Introduction to AC Machine Design*, 2 edition. Madison, WI: University of Wisconsin-Madison, 2007.

[4] J. Pyrhonen, T. Jokinen, and V. Hrabovcova, *Design of Rotating Electrical Machines*, 1 edition. Chichester, West Sussex, United Kingdom ; Hoboken, NJ: Wiley, 2009.

[5] N. L. Schmitz and D. W. Novotny, *Introductory Electromechanics*. Ronald Press, 1965.

[6] G. Kron, *Tensor Analysis of Networks*. Wiley, 1949.

[7] D. W. Novotny and T. A. Lipo, *Vector Control and Dynamics of AC Drives*, 1 edition. Oxford : New York: Clarendon Press, 1996.

[8] N. Bianchi and G. Berardi, "Analytical Approach to Design Hairpin Windings in High Performance Electric Vehicle Motors," in *2018 IEEE Energy Conversion Congress and Exposition (ECCE)*, Sep. 2018, pp. 4398–4405. doi: 10.1109/ECCE.2018.8558383.

[9] A. J. McConnell, *Applications of Tensor Analysis*. New York, NY: Dover Publications, 2011.

[10] D. Knuth, *Art of Computer Programming, The: Combinatorial Algorithms, Volume 4B*, 1st edition. Boston Columbus: Addison-Wesley Professional, 2022.